Appendix 3. Additional example figures

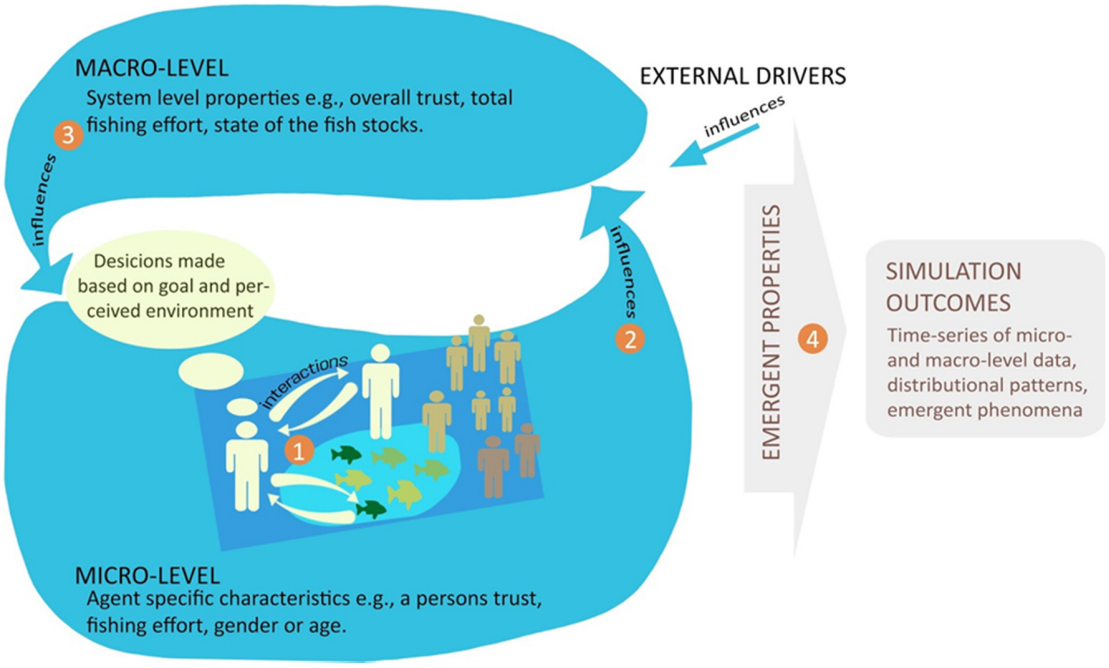

Fig. A3.1. Visualization of an agent-based fisheries SES model by a conceptual diagram. The focus is put on the interplay (reciprocal causal relationships) between agents' characteristics and (inter)actions (the micro-level) and system properties (the macro-level). This interplay is affected by environmental drivers and it causes emergent properties of the modeled system, both at the macro- and micro-level. Numbered markers are used to visually guide readers through the steps of micro- and macro-level changes affecting each other during the simulation. Different kinds of objects and arrows as well as labels and additional illustrations show and discriminate the processes operating during the simulation (left) and the emergent simulation outcomes (right). Source and further details: Lindkvist et al. (2020). Figure used without modification under the CC BY 4.0 license (https://creativecommons.org/licenses/by/4.0/).

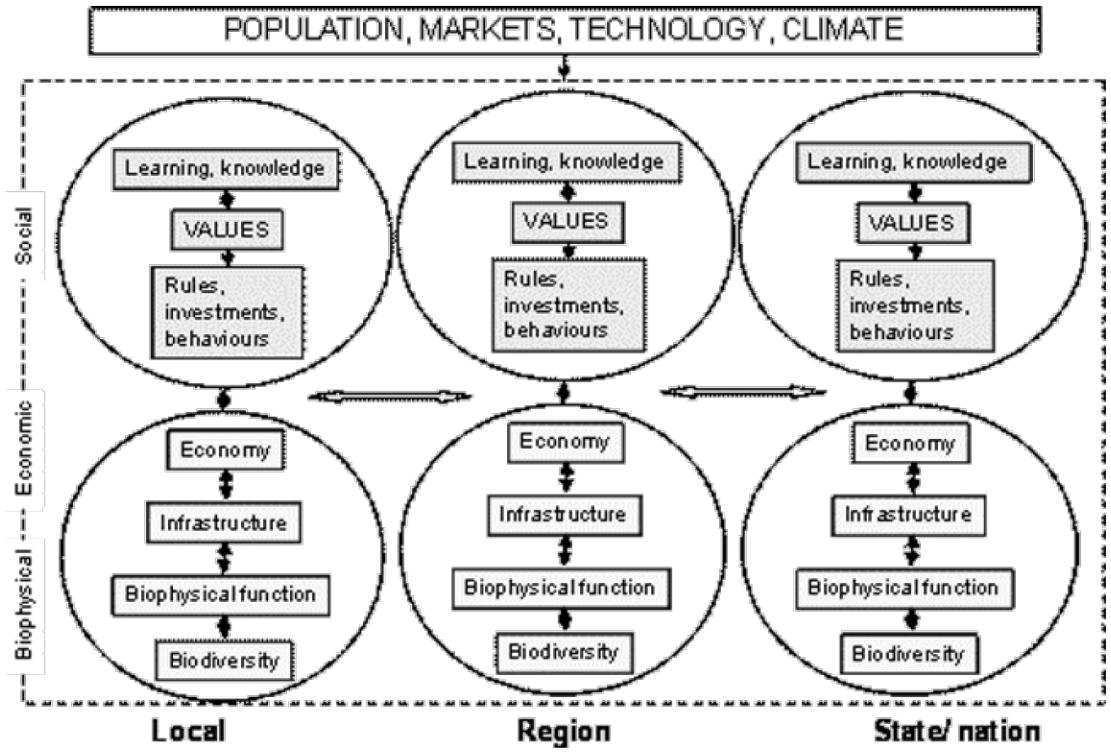

Fig. A3.2. Visualization of a framework for assessing the social-ecological resilience of a study region, using a large number of objects and arrows to represent complex causation. Resilience is assessed for multiple biophysical, economic and social values (left labels) and multiple spatial scales (bottom labels). Different variables driving the system's state are visualized by boxes, grouped in circles, and their multiple interactions shown by many arrows. Exogenous drivers of the SES state are visualized as an additional box linked by an arrow (top). Source and further details: Walker et al. (2009). Figure used without modification under the CC BY 4.0 license (https://creativecommons.org/licenses/by/4.0/).

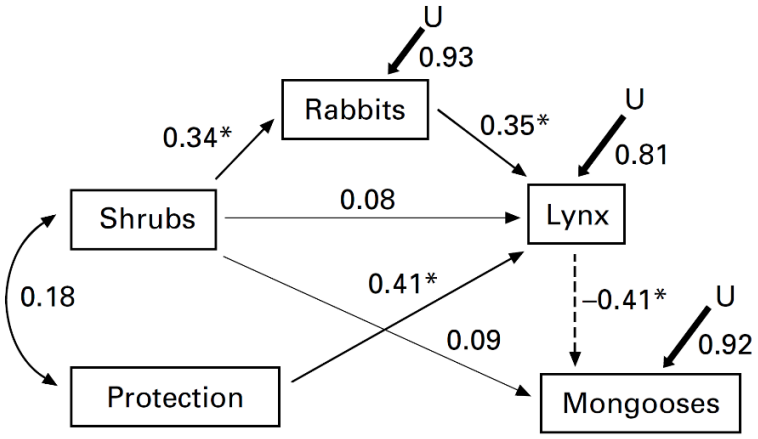

Fig. A3.3. Visualization of structural equation modeling (SEM) results for a Mediterranean ecosystem in south-western Spain by a causal diagram with a standard formalism. Path coefficients provide the strength and sign of statistical relationships between variables (additionally visualized by the thickness and line style of arrows, dashed for negative relationship). Relationships significantly different from zero are marked with an asterisk. Arrows pointing to a variable that do not start from another variable (marked with 'U') represent error terms in the SEM, which account for variance in those variables due to unmeasured causal factors or stochasticity. The additional curved arrow between two variables visualizes that no hypothesis on their causal relationship was included in the model. Their correlation might represent a causal relationship in any direction or effects of a common, unmeasured causal factor. Source and further details: Palomares et al. (1998). Figure used with permission by John Wiley and Sons.

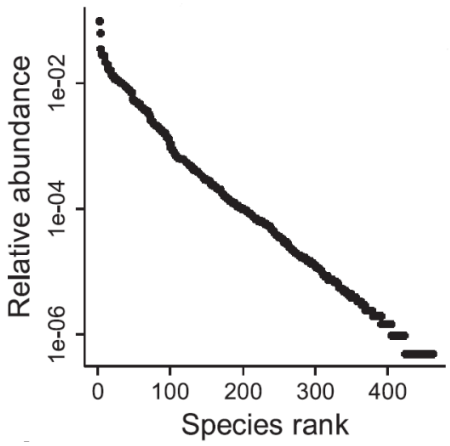

Fig. A3.4. Visualization of a simulated abundance distribution of tropical tree species by an X-Y-plot. The species are ranked (X-axis) according to their abundance, which is plotted relative to the total abundance of the community (Y-axis, logarithmic scale). The species ranks are the plain result of sorting and do not imply to be the cause for the depicted abundances. Source and further details: May et al. (2016). Figure used with permission by John Wiley and Sons.

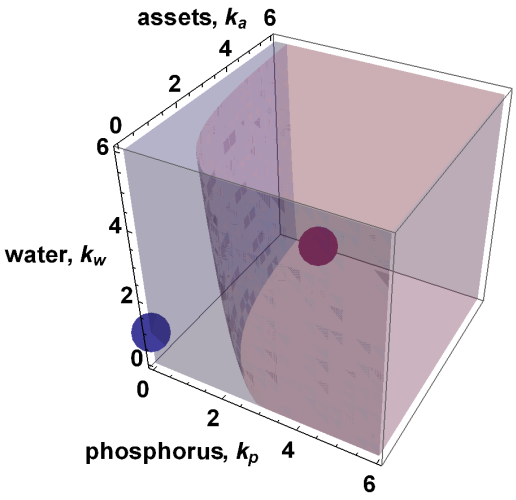

Fig. A3.5. Visualization of the state space of an agricultural SES by an X-Y-Z-plot. Three SES state variables are depicted that are all causally related to each other in a dynamical systems model: phosphorous in the environment (X-axis), household assets (Y-axis) and water level (Z-axis). Two colored circles visualize two different stable states the system can approach over time (attractors) and the transparent colored volumes separate the initial states that cause one or the other attractor to be reached (basins of attraction). Source and further details: Radosavljevic et al. (2020). Figure used in accordance with the authors' right to reuse own material (https://www.elsevier.com/about/policies/copyright).

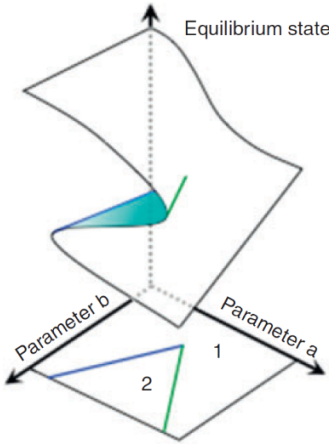

Fig. A3.6. Visualization of the so-called “cusp” model from catastrophe theory by an X-Y-Z-plot. The causal relationship between one variable (parameter a, X-axis) and the system’s equilibrium state (Z-axis) changes qualitatively depending on a second variable (parameter b, Y-axis). The bottom areas visualize the combinations of values of a and b with either one corresponding stable state (area 1) or two alternative stable states (area 2, i.e. hysteresis in the relationship between parameter a and the system state, cf. Fig. 5B in the main text). The transparent fold shows the possible system states, the cyan fold shows states that cannot be reached. Source and further details: Petraitis and Dudgeon (2016). Figure used with permission by CSIRO Publishing.

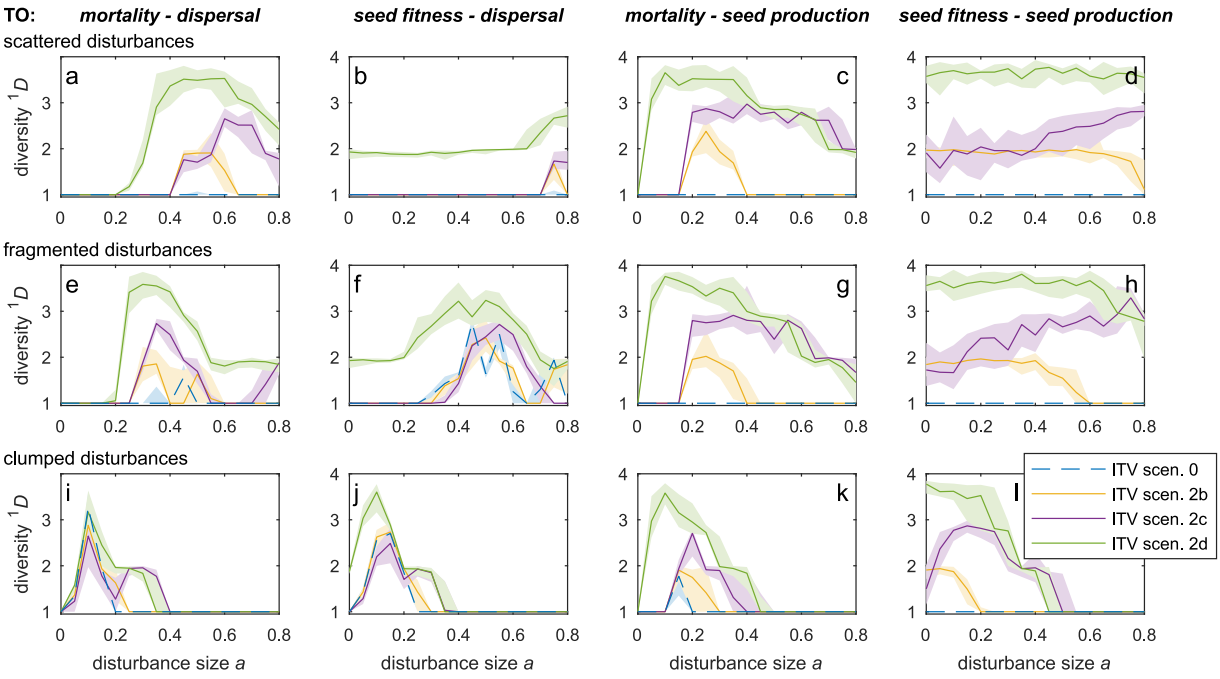

Fig. A3.7. Visualization of the effects of multiple factors on biodiversity in a modeled ecosystem by multiple X-Y-plots. In each subplot, the quantitative relationships between disturbance size (X-axes) and species diversity (Y-axes) are shown, with shaded areas visualizing the variation among multiple stochastic simulation runs. The additional factors causally related to diversity are the actual trade-off in species traits (TO, different columns), the spatial configuration of disturbances (different rows), and the applied scenario of intraspecific trait variation (ITV, different colors). Source and further details: Banitz (2019). Figure used in accordance with the authors' right to reuse own material (https://onlinelibrary.wiley.com/page/journal/16000706/homepage/Permissions.html).

		Total deaths			
R_0	On Trigger	Do nothing	CI_HQ_SD	PC_CI_SD	PC_CI_HQ_SD
2	60	410,000	47,000	6,400	5,600
	100	410,000	47,000	9,900	8,300
	200	410,000	46,000	17,000	14,000
	300	410,000	45,000	24,000	21,000
	400	410,000	44,000	30,000	26,000
2.2	60	460,000	62,000	9,700	6,900
	100	460,000	61,000	13,000	10,000
	200	460,000	64,000	23,000	17,000
	300	460,000	65,000	32,000	26,000
	400	460,000	68,000	39,000	31,000
2.4	60	510,000	85,000	12,000	8,700
	100	510,000	87,000	19,000	13,000
	200	510,000	90,000	30,000	24,000
	300	510,000	94,000	43,000	34,000
	400	510,000	98,000	53,000	39,000
2.6	60	550,000	110,000	20,000	12,000
	100	550,000	110,000	26,000	16,000
	200	550,000	120,000	39,000	30,000
	300	550,000	120,000	56,000	40,000
	400	550,000	120,000	71,000	48,000

Fig. A3.8. Visualization of the effects of multiple factors on death tolls in a human pandemic model by a colored table, which yields a nested raster plot in a simple manner. It shows the effects of the three causal factors intervention strategy (X-axis, different column labels), number of intensive care unit cases needed to trigger the intervention (inner Y-axis, range 60-400), and virus reproduction number R_0 (outer Y-axis, range 2-2.6) on the simulated number of total deaths (cell entries, visualized by color). Source and further details: Ferguson et al. (2020). Figure used without modification under the CC BY-NC-ND 4.0 license (https://creativecommons.org/licenses/by-nc-nd/4.0/).

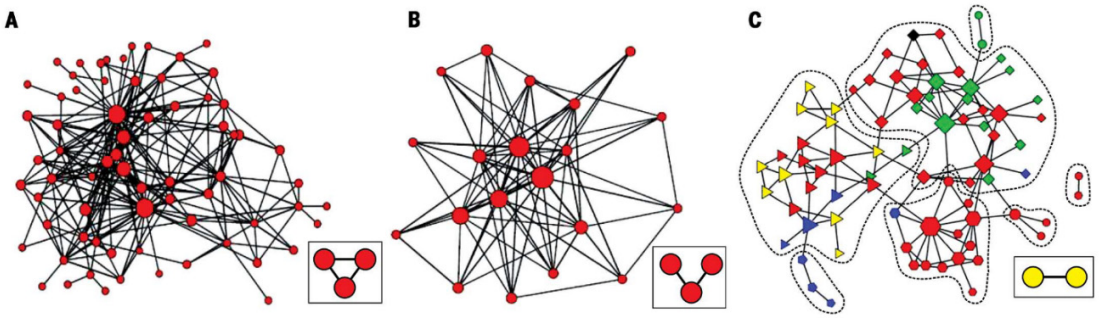

Fig. A3.9. Visualization of human collaboration in different SES by multiple network diagrams. The nodes depict human actors and the edges connect collaborating actors in (A) coastal ecosystem management in Sweden, (B) biosphere reserve management in Canada, and (C) small-scale coastal fishery in Kenya. In network C, different colors visualize different types of gear used by the fishers and dashed lines show different subgroups of fishers with many connections between them. The combination of multiple network diagrams in one figure facilitates comparison of the different networks' structural characteristics and causal interpretation of these structures (cf. Section 3.1.3 in the main text). Insets in the bottom right of each subplot show frequent structural building blocks of the visualized network, respectively. Source and further details: Bodin (2017). Figure used with permission by The American Association for the Advancement of Science.

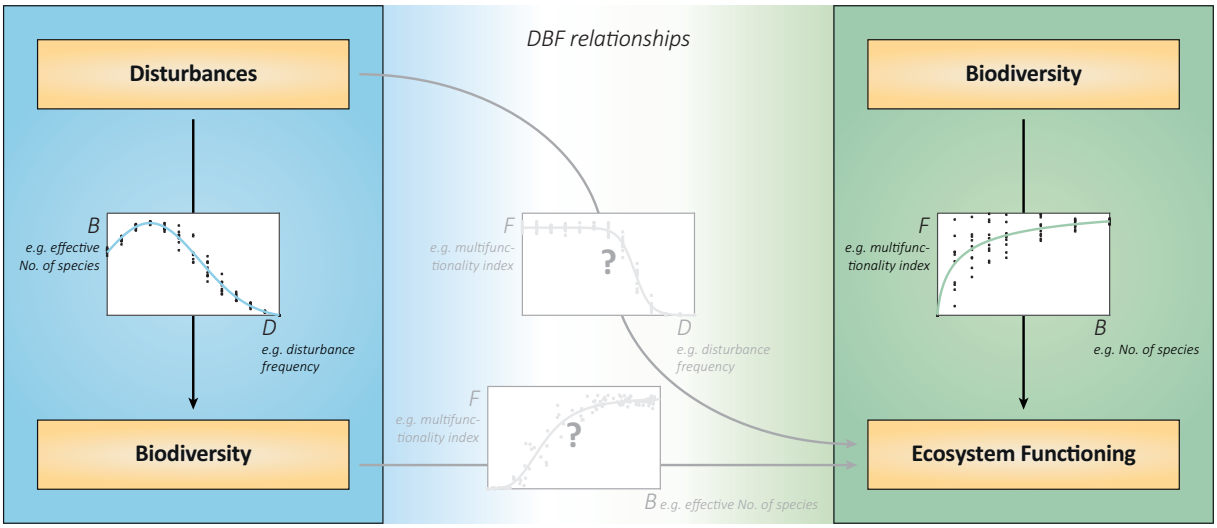

Fig. A3.10. Visualization of complex causation in a conceptual ecosystem model by combining a diagram of objects and arrows with X-Y-plots. The objects and arrows visualize causal relationships between disturbances D, biodiversity B and ecosystem functioning F (biodiversity is shown twice to illustrate that its relationship to ecosystem functioning is often studied separately from disturbances). The X-Y-plots inserted visualize observable relationships between variables representing the connected objects, respectively (axis labels). These emergent DBF relationships are affected by the underlying causal relationship between these variables, and by additional variables (either shown or not shown). For example, the relationship between the effective number of species and the multifunctionality index (bottom X-Y-plot) is confounded by the disturbance frequency which is causally related to both variables (visually detectable by a backdoor path between them, cf. Section 3.2.1 in the main text). Source and further details: Banitz et al. (2020). Figure used without modification under the CC BY 4.0 license (https://creativecommons.org/licenses/by/4.0/).

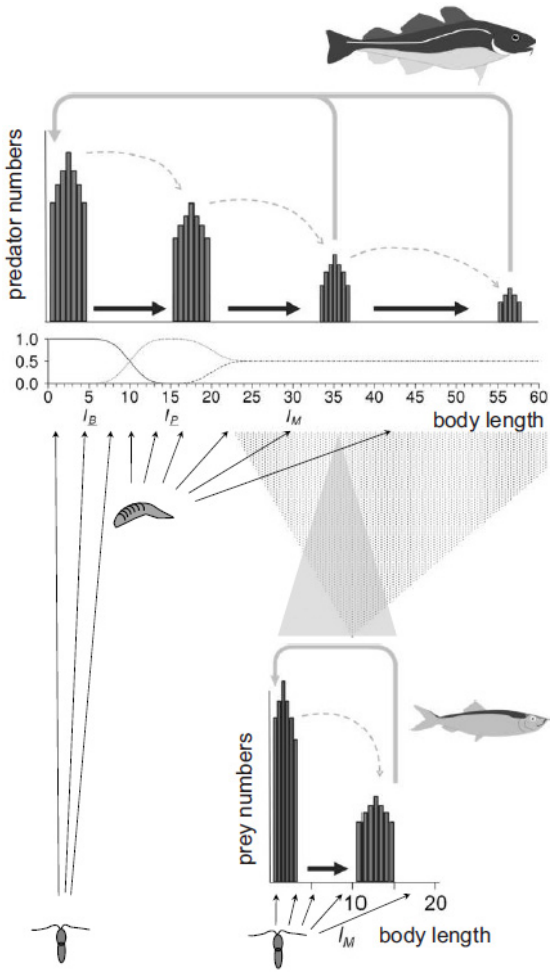

Fig. A3.11. Visualization of complex trophic relationships between different species in a marine ecosystem model by combining X-Y-plots with diagrams of objects and arrows. The two bar plots (X-Y-plots) visualize frequency distributions of body length (X-axes) of two fish species (the predator cod and the prey sprat, cf. Y-axes, also visualized by icons). They show that the populations are structured in cohorts. In these bar plots, arrows between cohorts visually indicate the model processes growth (black arrows), reproduction (gray arrows) and mortality (dashed gray arrows). Another line plot (X-Y-plot) visualizes the switching of cod prey preference throughout its life-stages. Additional prey species are visualized by icons (zooplankton at the bottom, benthic organisms in the middle), and thin arrows represent biomass flows from these prey species to the different life-stages of the two fish species. Similarly, the gray areas visualize the predator-prey relationship between the two fish species, but here the dotted area shows the size range of predators that can feed on a prey individual of a certain size (11 cm), and the shaded area shows the size range of prey a predator individual of a certain size (35 cm) can feed on. The figure requires detailed explanation, but helps understanding the model rules and processes that let the population dynamics emerge in simulations. Source and further details: van Leeuwen et al. (2013). Figure used with permission by the University of Chicago Press.

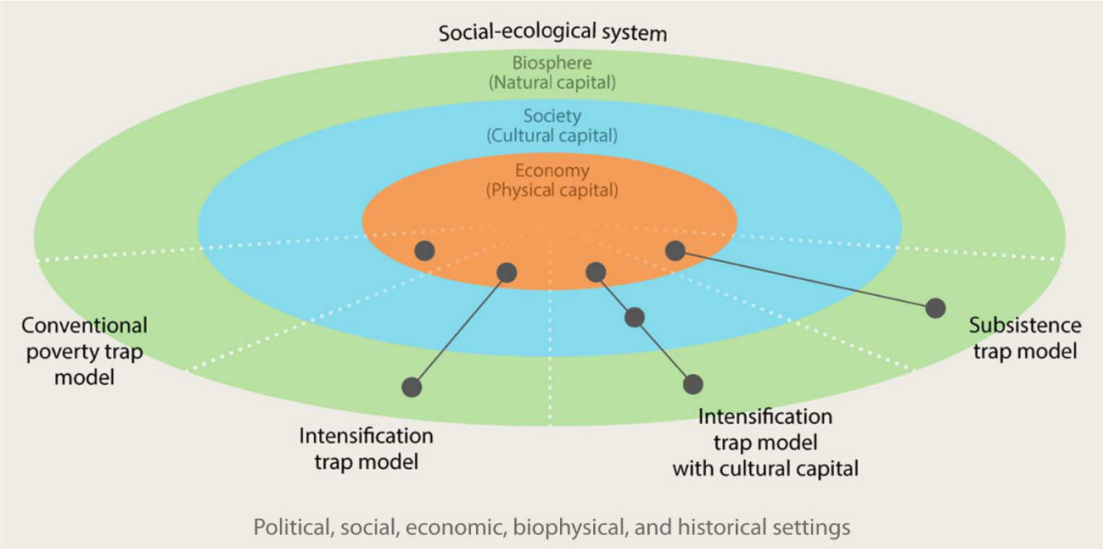

Fig. A3.12. Visualization of an SES conceptualization by a set diagram. The colored areas visualize that economy is considered a part of society and this society is considered a part of the biosphere (cf. Folke et al. 2016). Gray lines and circles depict different poverty trap models, which explicitly take into account different subsets of the complex SES. Source and further details: Lade et al. (2017). Figure used without modification under the CC BY 4.0 license (https://creativecommons.org/licenses/by/4.0/).

Literature cited

Banitz, T. 2019. Spatially structured intraspecific trait variation can foster biodiversity in disturbed, heterogeneous environments. *Oikos* 128(10):1478–1491.

Banitz, T., A. Chatzinotas, and A. Worrich. 2020. Prospects for integrating disturbances, biodiversity and ecosystem functioning using microbial systems. *Frontiers in Ecology and Evolution* 8.

Bodin, Ö. 2017. Collaborative environmental governance: achieving collective action in social-ecological systems. *Science* 357(6352):eaan1114.

Ferguson, N. M., D. Laydon, G. Nedjati-Gilani, N. Imai, K. Ainslie, M. Baguelin, S. Bhatia, A. Boonyasiri, Z. Cucunubá, and G. Cuomo-Dannenburg. 2020. Impact of non-pharmaceutical interventions (NPIs) to reduce COVID-19 mortality and healthcare demand. Imperial College COVID-19 Response Team. *Imperial College COVID-19 Response Team*:20.

Folke, C., R. Biggs, A. V. Norström, B. Reyers, and J. Rockström. 2016. Social-ecological resilience and biosphere-based sustainability science. *Ecology and Society* 21(3).

Lade, S. J., L. J. Haider, G. Engström, and M. Schlüter. 2017. Resilience offers escape from trapped thinking on poverty alleviation. *Science Advances* 3(5):e1603043.

van Leeuwen, A., M. Huss, A. Gårdmark, M. Casini, F. Vitale, J. Hjelm, L. Persson, and A. M. de Roos. 2013. Predators with multiple ontogenetic niche shifts have limited potential for population growth and top-down control of their prey. *The American Naturalist* 182(1):53–66.

Lindkvist, E., N. Wijermans, T. M. Daw, B. Gonzalez-Mon, A. Giron-Nava, A. F. Johnson, I. van Putten, X. Basurto, and M. Schlüter. 2020. Navigating complexities: agent-based modeling to support research, governance, and management in small-scale fisheries. *Frontiers in Marine Science* 6.

May, F., T. Wiegand, S. Lehmann, and A. Huth. 2016. Do abundance distributions and species aggregation correctly predict macroecological biodiversity patterns in tropical forests? *Global Ecology and Biogeography* 25(5):575–585.

Palomares, F., P. Ferreras, A. Travaini, and M. Delibes. 1998. Co-existence between Iberian lynx and Egyptian mongooses: estimating interaction strength by structural equation modelling and testing by an observational study. *Journal of Animal Ecology* 67(6):967–978.

Petraitis, P. S., and S. R. Dudgeon. 2016. Cusps and butterflies: multiple stable states in marine systems as catastrophes. *Marine and Freshwater Research* 67(1):37–46.

Radosavljevic, S., L. J. Haider, S. J. Lade, and M. Schlüter. 2020. Effective alleviation of rural poverty depends on the interplay between productivity, nutrients, water and soil quality. *Ecological Economics* 169:106494.

Walker, B. H., N. Abel, J. M. Anderies, and P. Ryan. 2009. Resilience, adaptability, and transformability in the Goulburn-Broken catchment, Australia. *Ecology and Society* 14(1):art12.